



Scholars Research Library

Der Pharma Chemica, 2010, 2(6): 243-255
(<http://derpharmachemica.com/archive.html>)



Pharmacophore modeling and 3D QSAR studies on Chalcones as *Trypanosoma cruzi* inhibitors

Jyoti¹*, Sukhbir L. Khokra¹ and A. Husain²

*Institute of Pharmaceutical Sciences, Kurukshetra University, Kurukshetra – 136 119, Haryana¹
Department of Pharmaceutical Sciences, Jamia Hamdard, Hamdard nagar, New Delhi²*

ABSTRACT

*In order to understand the essential structural features for chalcones as *Trypanosoma cruzi* inhibitors, three-dimensional pharmacophore hypothesis were built on the basis of a set of known *Trypanosoma cruzi* inhibitors selected from literature using PHASE program. Five point pharmacophore with three hydrogen bond acceptor (A), and two aromatic ring (R) as pharmacophoric features were developed. Amongst them the pharmacophore hypothesis AAARR11 yielded a statistically significant 3D-QSAR model with 0.9371 as R^2 value and was considered to be the best pharmacophore hypothesis. The developed pharmacophore model was externally validated by predicting the activity of test set molecules. The squared predictive correlation coefficient of 0.870 was observed between experimental and predicted activity values of test set molecules. The geometry and features of pharmacophore were expected to be useful for the design of selective *Trypanosoma cruzi* inhibitors.*

Keywords: 3D-QSAR, pharmacophore hypothesis, regression coefficient, squared predictive correlation coefficient.

INTRODUCTION

Chalcones possess a broad spectrum of biological activities like antioxidative, antibacterial, antihelmintic, amoebicidal, antiulcer, antiviral, insecticidal, antiprotozoal, anticancer, cytotoxic & immunosuppressive activities [1]. In 2000, only about 0.1% of global investment in health research was devoted to drug discovery for selected tropical diseases like malaria, leishmaniasis, trypanosomiasis and tuberculosis, which together contribute about 5% of global disease burden [2]. Some trypanocidal drugs as Nifurtimox & benznidazole act through free radical generation. *T. cruzi* is very susceptible to cell damage, because enzymes scavenging free radical are absent or have very low activities in the parasite [3].

The pharmacophore modeling is a well established approach to quantitatively explore common chemical features among a considerable number of structures and qualified pharmacophore model could also be used as a query for searching chemical databases to find new chemical entities. Pharmacophore modeling correlates activities with the spatial arrangement of various chemical features [4]. Ligand-based drug design approaches like pharmacophore mapping [5] and quantitative structure-activity relationship [6,7] can be used in drug discovery in several ways, e.g. rationalization of activity trends in molecules under study, prediction of the activity of novel compounds, database search studies in search of new hits and to identify important features for activity.

This paper describes the development of a robust ligand-based 3D-pharmacophore hypothesis. The pharmacophore hypothesis obtained from the pharmacophoric points is used to derive pharmacophore - based 3D-QSAR model. Such a pharmacophore model provides a rational hypothetical picture of primary chemical features responsible for activity [8].

MATERIALS AND METHODS

Dataset

The *in-vitro* biological data [9] of a series of 28 compounds having *Trypanosoma cruzi* inhibitory activity was used for the present studies. The *Trypanosoma cruzi* inhibitory activity was expressed as IC₅₀ i.e., concentration in μm required for 50% inhibition of enzyme activity. The dataset was divided randomly into training set and test set by considering the 75% of the total molecules in the training set and 25% in the test set. Twenty one molecules forming the training set were used to generate pharmacophore models and prediction of the activity of test set (7analogues) molecules was used as a method to validate the proposed models.

Pharmacophore modeling

Pharmacophore modeling and 3-D database searching are now recognized as integral components of lead discovery and lead optimization. The continuing need for improved pharmacophore based tools has driven the development of 'PHASE' [10]. To reach our research objectives we have used 'PHASE' a module of Schrödinger's software program 'MAESTRO' [11].

Ligand Preparation

The first step for pharmacophore modeling studies was ligand preparation. The chemical structures of all the compounds were drawn in maestro and geometrically refined using Ligprep module. *LigPrep* is a robust collection of tools designed to prepare high quality, all-atom 3D structures for large numbers of drug-like molecules, starting with the 2D or 3D structures in SD or Maestro format. The simplest use of LigPrep produces a single, low-energy, 3D structure with correct chiralities for each successfully proposed input structure. While performing this step, chiralities were determined from 3D structure and original states of ionization were retained. Tautomers were generated using MacroModel method discarding current conformers. The conformations were generated by the Monte Carlo (MCMM) method as implemented in MacroModel version 9.6 using a maximum of 2,000 steps with a distance-dependent dielectric solvent model and an OPLS-2005 force field. All the conformers were subsequently minimized using truncated Newton conjugate gradient (TNCG) minimization up to 500 iterations. For each molecule, a set of conformers with a maximum energy difference of 30kcal/mol relative to the global energy minimum conformer was retained. The conformational searches were done for aqueous solution using the generalized born/solvent accessible surface (GB/SA) continuum solvation model [12].

Creation of Pharmacophoric Sites

The next second step in developing a pharmacophore model is to use a set of pharmacophore features to create pharmacophore sites (site points) for all the ligands. In the present study, an initial analysis revealed that two chemical feature types i.e., hydrogen-bond acceptor (A), and aromatic ring (R) could effectively map all critical chemical features of all molecules in the data set. The minimum and maximum sites for all the features were kept 3 and 5 respectively. These features were selected and used to build a series of hypothesis with the find common pharmacophore option in Phase.

Searching Common Pharmacophore

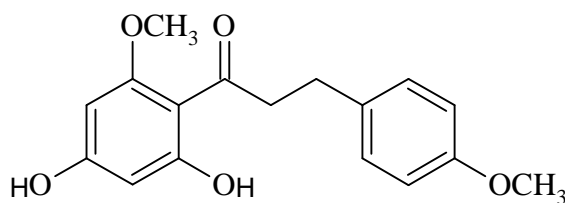
In this step, pharmacophores from all conformations of the ligands in the data set were examined and those pharmacophores that contain identical sets of features with very similar spatial arrangements were grouped together. If a given group is found to contain at least one pharmacophore from each ligand, then this group gives rise to a common pharmacophore. Any single pharmacophore in the group could ultimately become a common pharmacophore hypothesis. Common pharmacophores are identified using a tree - based partitioning technique that groups together similar pharmacophores according to their inter site distances, i.e., the distances between pairs of sites in the pharmacophore.

Scoring Hypothesis

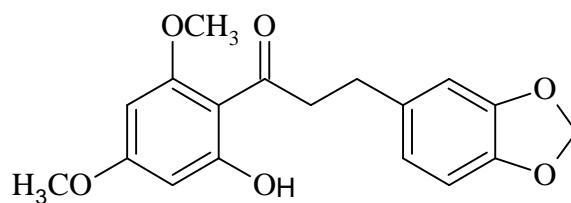
In this step, common pharmacophore hypothesis were examined using a scoring function to yield the best alignment of the active ligands using an overall maximum root mean square deviation (RMSD) value of 1.2 Å for distance tolerance. The quality of alignment was measured by survival score [13].

Generation of 3D-QSAR Model

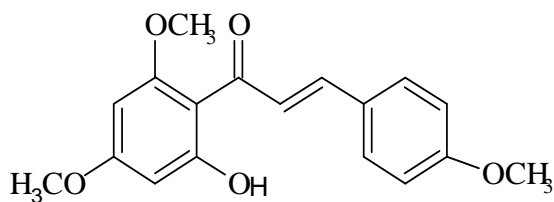
Phase provides the means to build 3D QSAR models for a set of ligands that are aligned to a selected hypothesis. The Phase 3D QSAR model partitions the space occupied by the ligands into a cubic grid. Any structural component can occupy part of one or more cubes. A cube is occupied by a feature if its centroid is within the radius of the feature. We can set the size of the cubes by changing the value in the Grid spacing text box. The regression is done by constructing a series of models with an increasing number of PLS factors. In present case, the pharmacophore based model was generated by keeping 1Å grid spacing and 3 as maximum number of PLS factors.



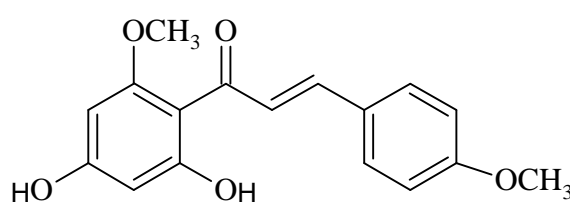
I



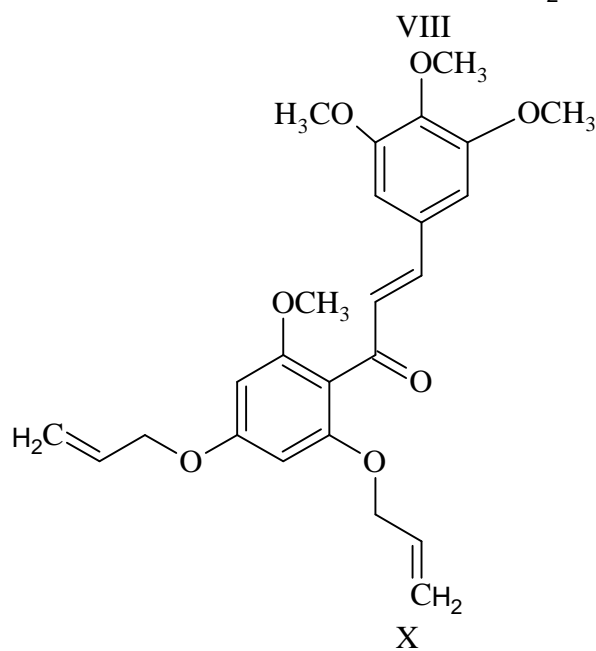
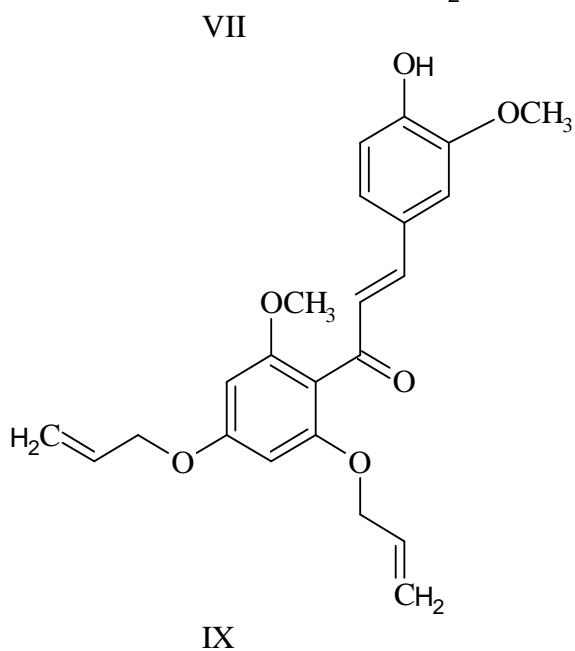
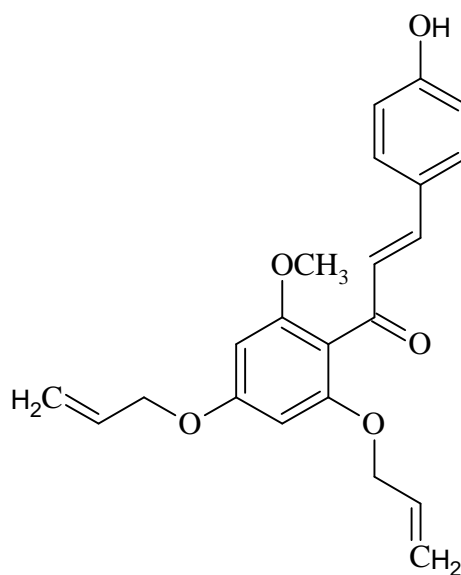
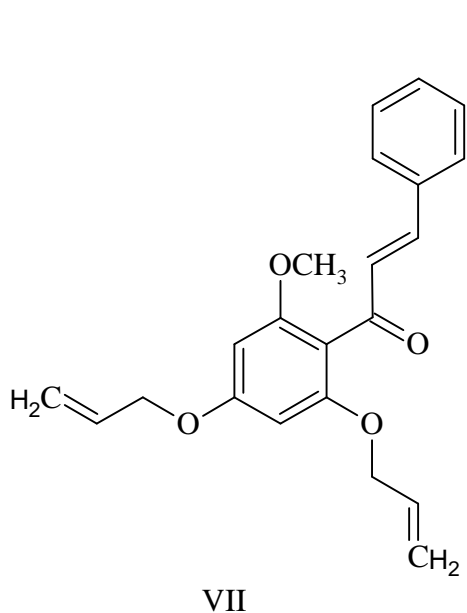
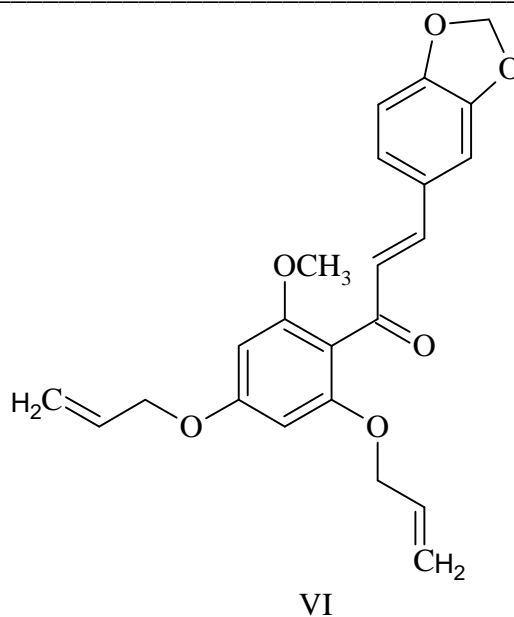
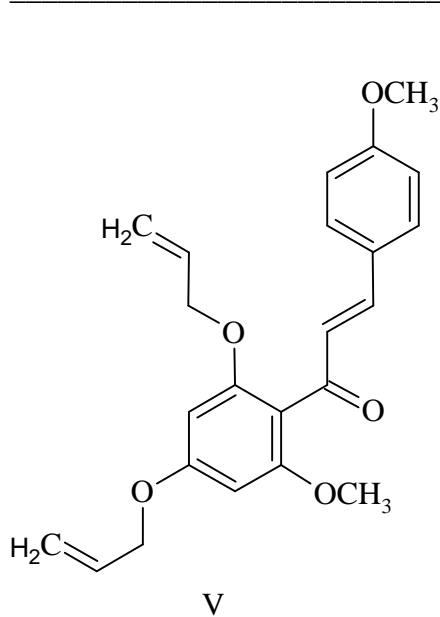
II

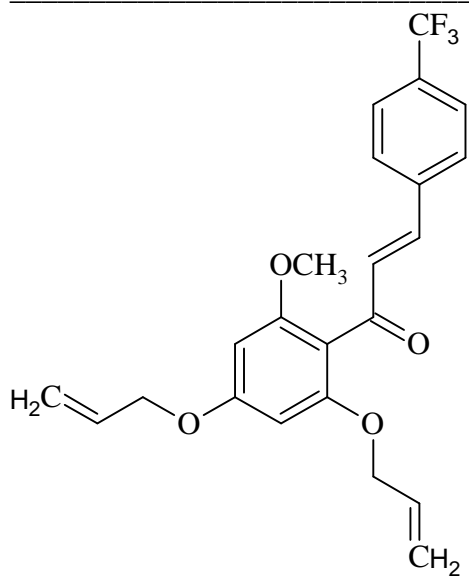


III

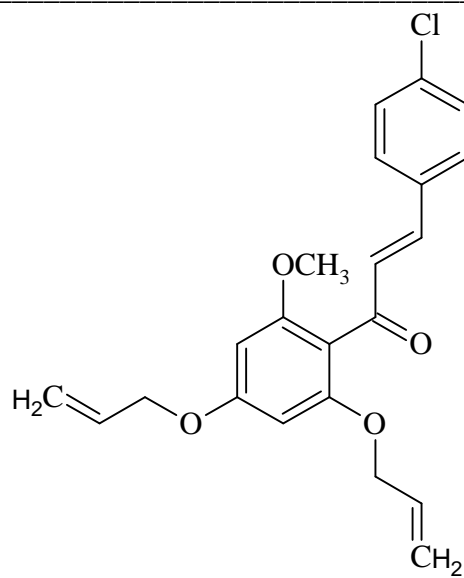


IV

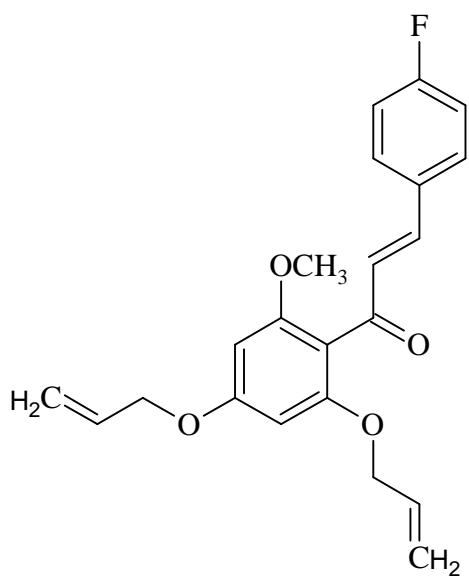




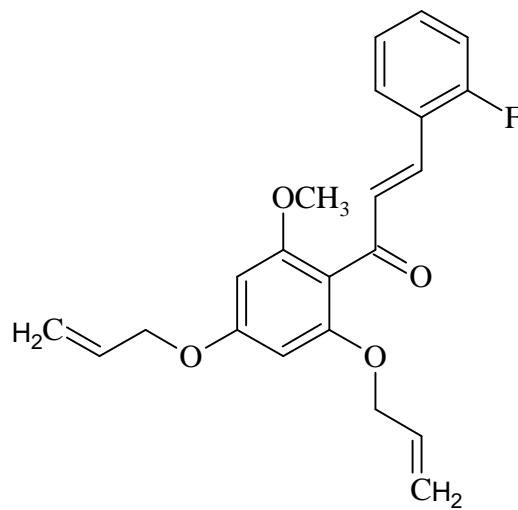
XI



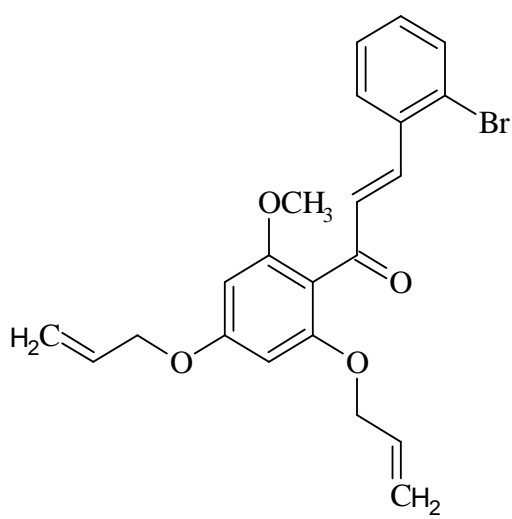
XII



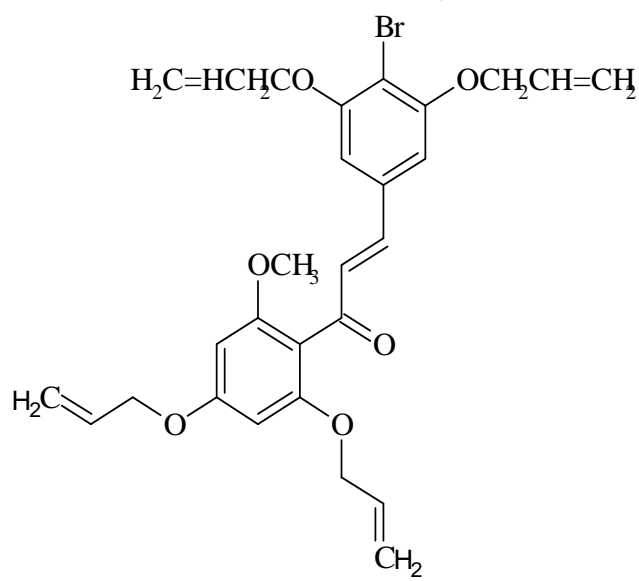
XIII



XIV



XV



XVI

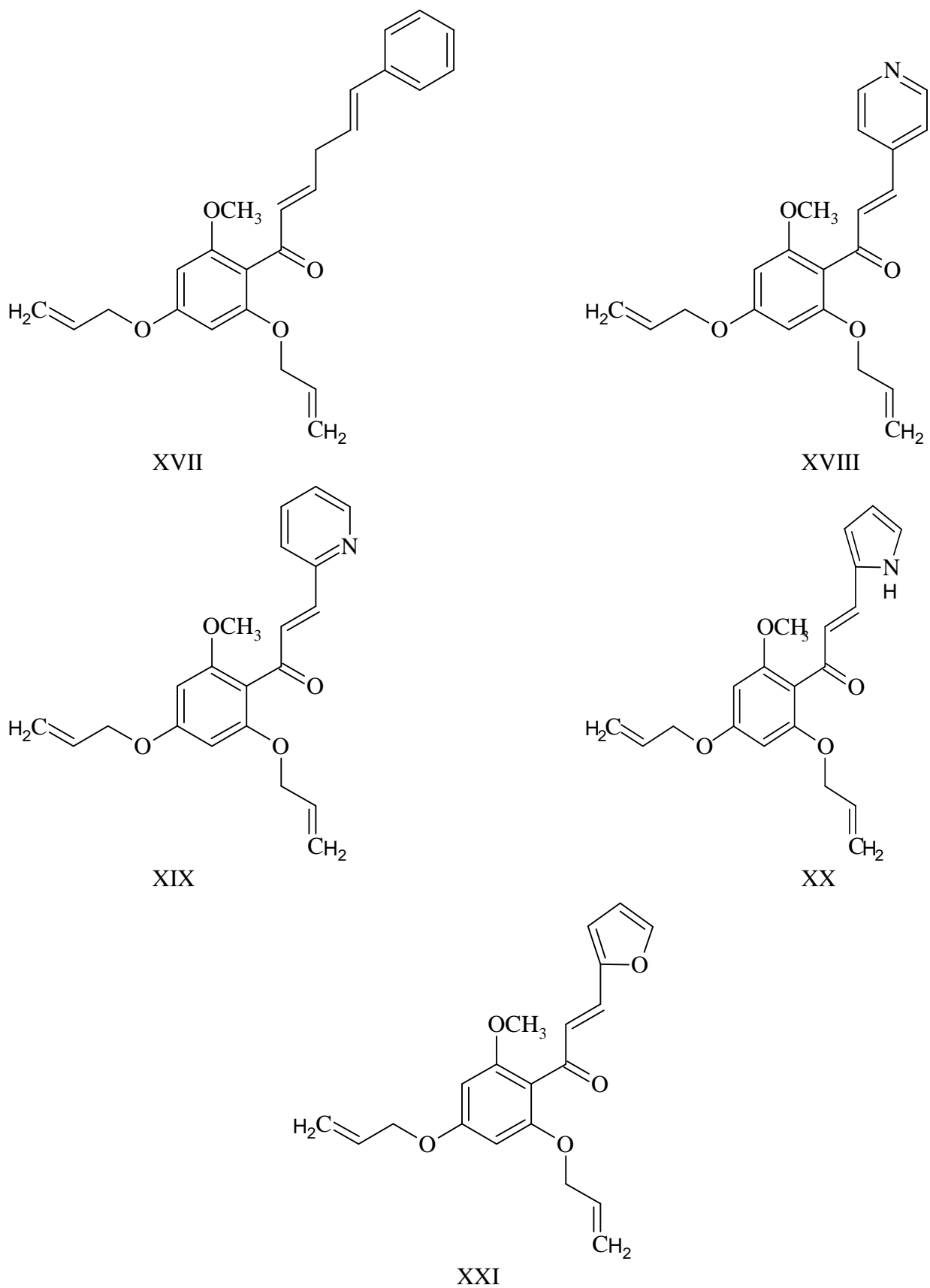


Figure 1: Chemical structures of the 21 training set molecules

Validation of Pharmacophore Model

Validation is a crucial aspect of pharmacophore design, particularly when the model is built for the purpose of predicting activities of compounds in external test series [14]. External validation is considered to be a conclusive proof for judging predictability of a model. Our priority was to develop QSAR models that were statistically robust both internally as well as externally. The main target of any QSAR modeling is that the developed model should be robust enough to be capable of making accurate and reliable predictions of biological activities of new compounds. In the present case, the developed pharmacophore model was validated by predicting the activity of test set molecules and correlation between the experimental and predicted activities of the test set molecules was determined.

RESULTS AND DISCUSSION

The purpose of pharmacophore modeling is to perform *in silico* screening searches in a 3 dimensional database of a virtual or real compound library to find diverse structures with desired binding activity and selectivity [15]. In the present study, a series of chalcones was considered for molecular modeling studies. The studies were aimed at developing a ligand based pharmacophore model relating the *Trypanosoma* inhibitory activity of chalcones to gain better understanding of ligand –*Trypanosoma* inhibitor interaction.

Twenty one molecules forming the training set were used to develop the pharmacophores. The pharmacophoric features selected for creating sites were hydrogen bond acceptor (A), and aromatic rings(R). Pharmacophore models containing three, four and five sites, i.e., features were generated. The three and four featured pharmacophore hypothesis were rejected due to low value of survival score, as they were unable to define the complete binding space of the selected molecules. Five featured pharmacophore hypothesis was selected and subjected to stringent scoring function analysis.

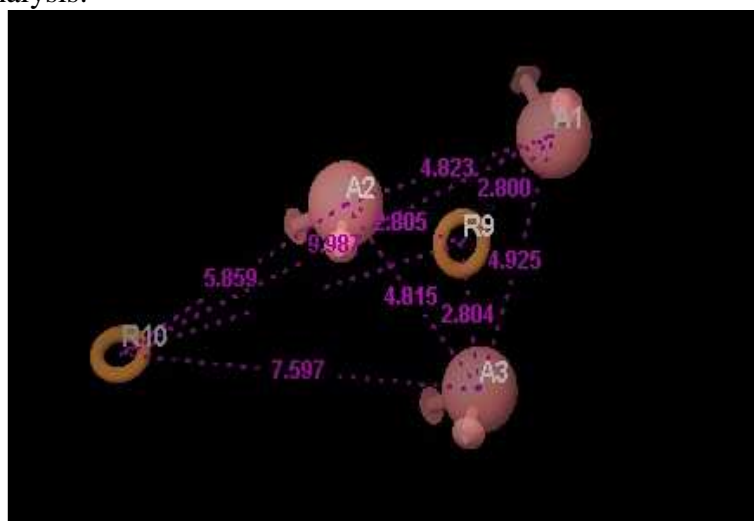


Figure 2: PHASE generated pharmacophore model AAARR11 illustrating hydrogen bond acceptor (A1, A2, A3; pink), and aromatic ring (R9;R10; orange) features with distances (in Å) between different sites of AAARR11

The result of (best) five featured pharmacophore hypothesis, labelled AAARR11 is shown in Table 1. The hypothesis AAARR11 was the best hypothesis in this study, characterized by highest survival score. The AAARR11 pharmacophore hypothesis is presented in Figure 1. The features represented by this hypothesis are two hydrogen bond acceptor (A), and one aromatic

ring(R). The distances and angles between different sites of AAARR11 are given in Table 2 and 3 respectively.

Table 1: Parameters of best five featured pharmacophore hypothesis

| S.No. | Hypothesis | Survival Score | R ² | F |
|-------|------------|----------------|----------------|------|
| 1 | AAARR11 | 3.422 | 0.9371 | 84.5 |

Table 2: Distances between different pharmacophoric sites of model AAARR11

| Site1 | Site2 | Distance(Å) | Site1 | Site2 | Distance(Å) |
|-------|-------|-------------|-------|-------|-------------|
| A3 | A2 | 4.815 | A2 | R9 | 2.805 |
| A3 | A1 | 4.925 | A2 | R10 | 5.859 |
| A3 | R9 | 2.804 | A1 | R9 | 2.800 |
| A3 | R10 | 7.597 | A1 | R10 | 9.987 |
| A2 | A1 | 4.823 | R9 | R10 | 7.520 |

Table 3: Angles between different pharmacophoric sites of model AAARR11

| Site1 | Site2 | Site3 | Angle | Site1 | Site2 | Site3 | Angle |
|-------|-------|-------|-------|-------|-------|-------|-------|
| A2 | A3 | A1 | 59.3 | A2 | A1 | R9 | 30.7 |
| A2 | A3 | R9 | 30.9 | A2 | A1 | R10 | 23.0 |
| A2 | A3 | R10 | 50.5 | R9 | A1 | R10 | 24.2 |
| A1 | A3 | R9 | 28.5 | A3 | R9 | A2 | 118.3 |
| A1 | A3 | R10 | 103.7 | A3 | R9 | A1 | 123.0 |
| R9 | A3 | R10 | 77.8 | A3 | R9 | R10 | 80.9 |
| A3 | A2 | A1 | 61.5 | A2 | R9 | A1 | 115.7 |
| A3 | A2 | R9 | 30.9 | A2 | R9 | R10 | 44.5 |
| A3 | A2 | R10 | 90.2 | A1 | R10 | R10 | 147.1 |
| A1 | A2 | R9 | 30.6 | A3 | R10 | A2 | 39.3 |
| A1 | A2 | R10 | 138.2 | A3 | R10 | A1 | 28.6 |
| R9 | A2 | R10 | 115.9 | A3 | R10 | R9 | 21.4 |
| A3 | A1 | A2 | 59.2 | A2 | R10 | A1 | 18.8 |
| A3 | A1 | R9 | 28.5 | A2 | R10 | R9 | 19.6 |
| A3 | A1 | R10 | 47.6 | A1 | R10 | R9 | 8.8 |

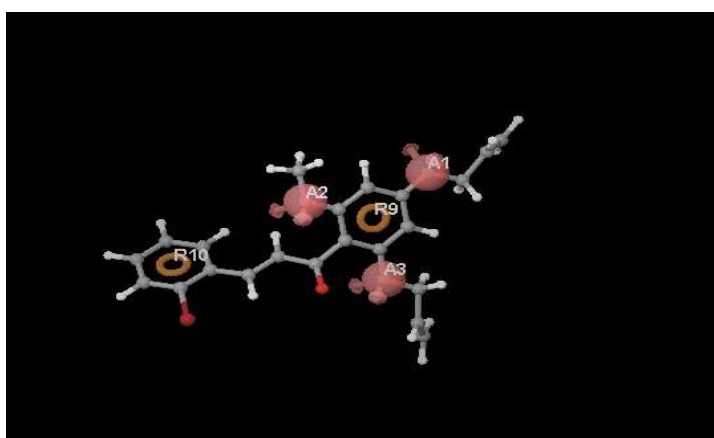


Figure 3: Best pharmacophore model AAARR11 aligned with molecule 21. Pharmacophore features are color coded: hydrogen bond acceptor (A1, A2, A3; pink), and aromatic ring (R9, R10; orange)

| Comp.No. | Experimental Activity IC ₅₀ (μ m) | Predicted Activity IC ₅₀ (μ m) | Fitness Score | Comp. No. | Experimental Activity(IC ₅₀) | Predicted Activity (IC ₅₀) | Fitness Score |
|----------|---|--|---------------|-----------|--|--|---------------|
| 1 | 26 | 19.84 | 1.97 | 12 | 8.6 | 3.77 | 2.62 |
| 2 | 101 | 100.14 | 2.40 | 13 | 14.3 | 6.75 | 2.87 |
| 3 | 26 | 33.71 | 2.63 | 14 | 6.2 | 8.09 | 2.64 |
| 4 | 26 | 27.17 | 2.58 | 15 | 13.9 | 15.70 | 3 |
| 5 | 21.4 | 9.27 | 2.84 | 16 | 6.9 | 7.97 | 2.71 |
| 6 | 13.6 | 13.4 | 2.54 | 17 | 26 | 36.22 | 1.69 |
| 7 | 17.1 | 14.80 | 2.10 | 18 | 1.5 | 7.43 | 2.91 |
| 8 | 20.3 | 13.22 | 2.58 | 19 | 1.9 | 9.90 | 2.75 |
| 9 | 26 | 21.37 | 1.96 | 20 | 101 | 93.88 | 2.57 |
| 10 | 3.4 | 3.21 | 2.42 | 21 | 12.2 | 27.64 | 2.77 |
| 11 | 15.6 | 18.63 | 2.17 | | | | |

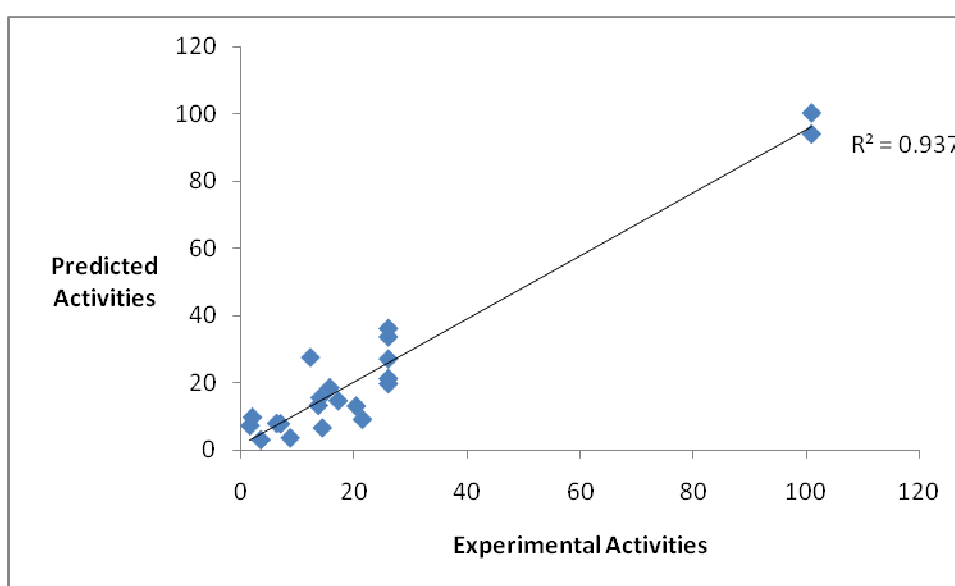


Figure 4: Relation between experimental and predicted Trypanosoma cruzi inhibitory activity values of training set molecules using model AAARR11.

The validity and predictive character of AAARR11 were further assessed by using the test set prediction. The test set having eight molecules was analyzed. All the test set molecules were built and minimized as well as used in conformational analysis like all training set molecules. Then the activities of test set molecules were predicted using AAARR11 and compared with the actual activity. Actual and predicted activity values of test set molecules are given in Table 5.

The predicted Trypanosoma cruzi inhibitory activity of test molecule exhibited a correlation of 0.870 with reported Trypanosoma cruzi inhibitory activity using model AAARR11 (Figure 6). For a reliable model, the squared predictive correlation coefficient should be >0.60 [16,17]. The results of this study reveal that model AAARR11 can be used for the prediction of Trypanosoma cruzi inhibitory activity.

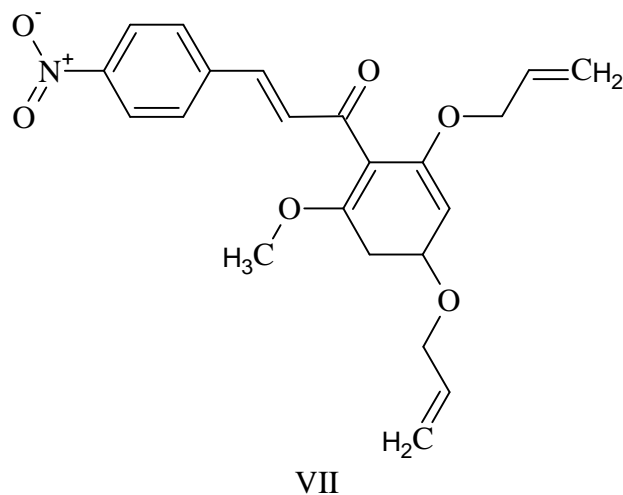
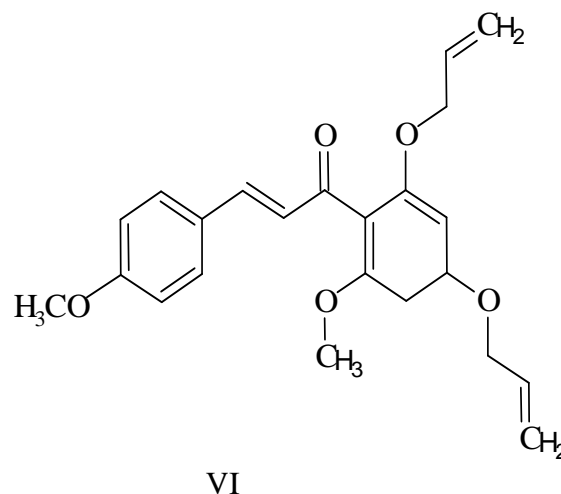
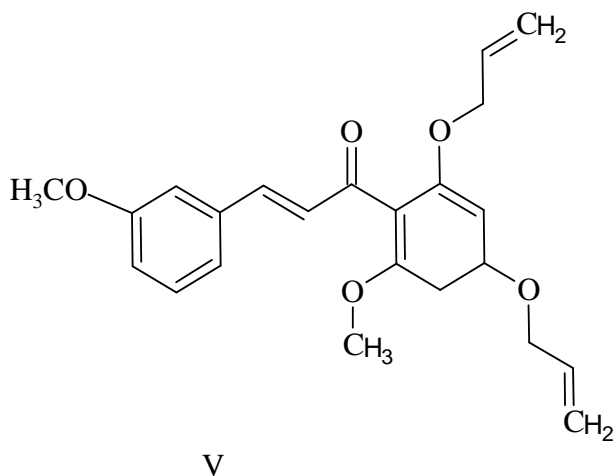
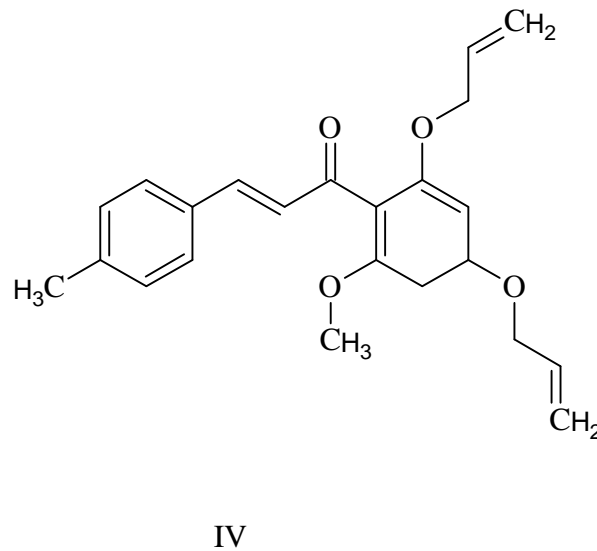
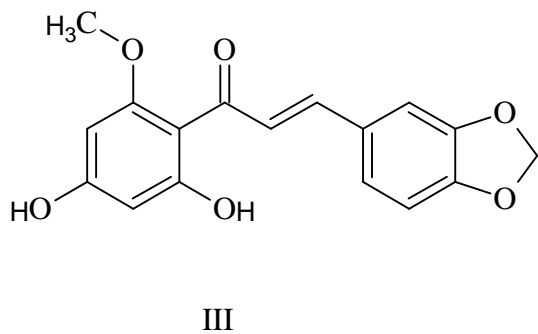
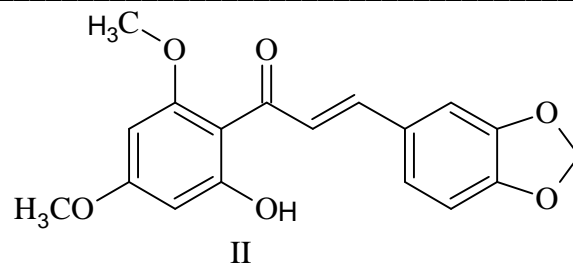
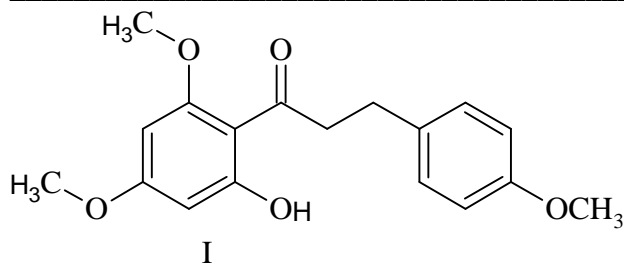
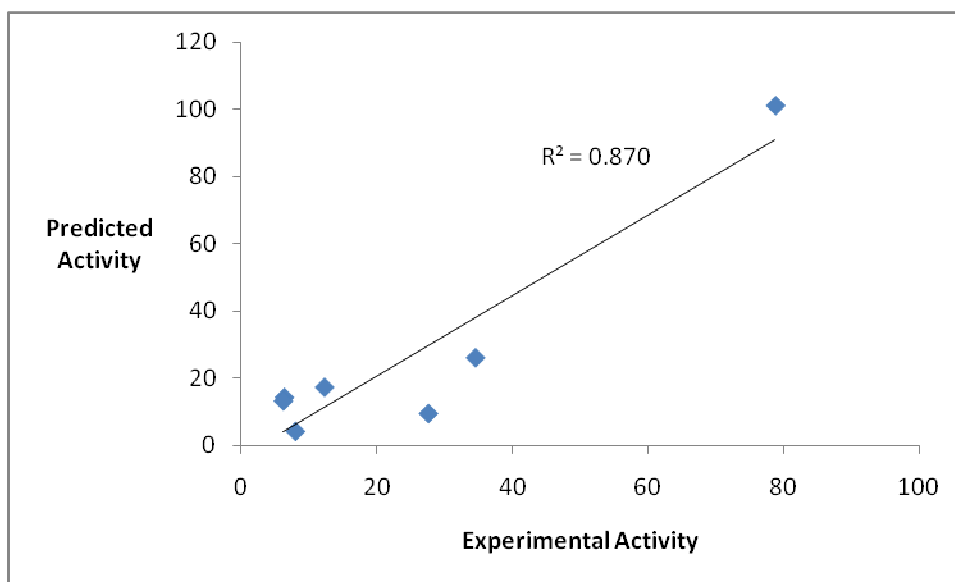


Table 6: Experimental and predicted activity of test molecules based on hypothesis AAARR11

| Comp.No. | Experimental Activity IC ₅₀ (μ m) | Predicted Activity IC ₅₀ (μ m) | Fitness Score | Comp.No. | Experimental Activity(IC ₅₀) | Predicted Activity(IC ₅₀) | Fitness Score |
|----------|---|--|---------------|----------|--|---------------------------------------|---------------|
| 1 | 101 | 78.77 | 2.40 | 5 | 14.2 | 6.33 | 2.15 |
| 2 | 26 | 34.51 | 2.62 | 6 | 13.1 | 6.17 | 2.76 |
| 3 | 9.4 | 27.57 | 2.58 | 7 | 4.1 | 7.95 | 2.82 |
| 4 | 17.2 | 12.24 | 2.76 | | | | |

Figure 3: Relation between experimental and predicted *Trypanosoma cruzi* inhibitory activity values of test set molecules using model AAARR11

3D QSAR Analysis

Additional insight into the *Trypanosoma cruzi* inhibitory activity can be gained by visualizing the 3D-QSAR model in the context of one or more ligands in the series with varying activity. This information can then be used to design new or more active analogues. 3-D QSAR models based on the molecules of training and test set using various features, i.e., hydrogen bond donor, hydrogen bond acceptors and aromatic ring has been studied.

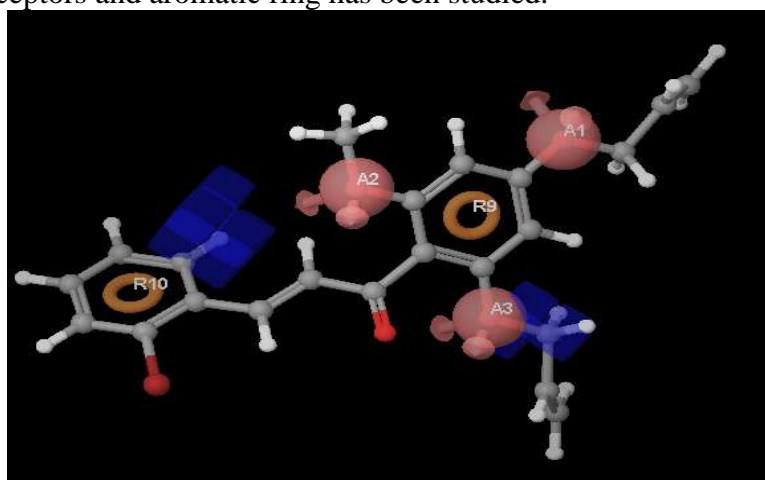


Figure 7: 3-D QSAR model based on molecule 21 of training set illustrating hydrogen bond donor feature

Blue region at meta position of phenyl ring substituted by bromo atom and at carbon of allyloxy group shows that if these positions will be occupied by any hydrogen bond donar that results in increase in activity.

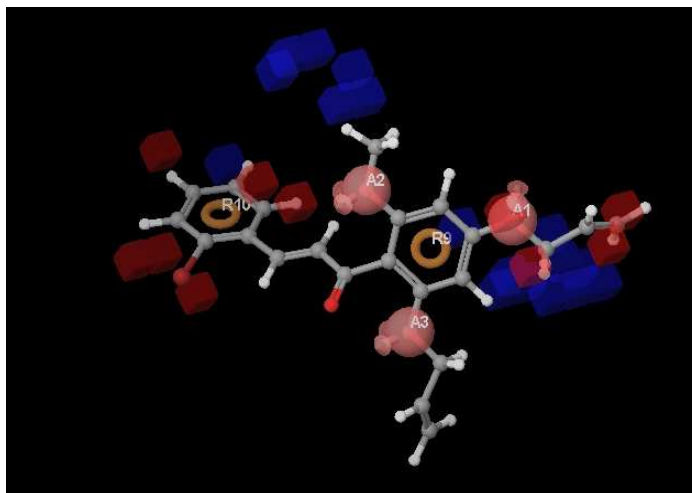


Figure 9: 3-D QSAR model based on molecule 21 of training set illustrating hydrophobic Feature

Red region at meta and para to bromo of phenyl ring shows that if these positions will be occupied by any hydrophobic group that results in decreasing activity.

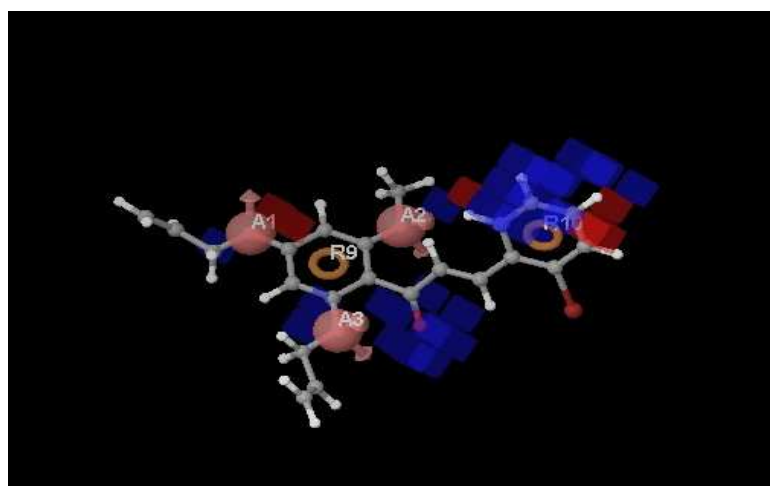


Figure 8: 3-D QSAR model based on molecule 21 of training set illustrating hydrogen bond acceptor feature

If blue region at carbonyl oxygen and at meta and para to bromo atom of phenyl ring will be occupied by any hydrogen bond acceptor resulting in increasing activity.

CONCLUSION

The studies shows the generation of a pharmacophore model AAARR11 compounds acting as *Trypanosoma cruzi* inhibitors. Pharmacophore modeling correlates activities with the spatial arrangement of various chemical features. Hypothesis AAARR11 represents the best pharmacophore model for determining *Trypanosoma cruzi* inhibitory activity. AAARR11 consists of three hydrogen bond acceptor, and two aromatic ring features. This pharmacophore model was able to accurately predict *Trypanosoma cruzi* inhibitory activity and the validation results also provide additional confidence in the proposed pharmacophore model. Results

suggested that the proposed 3-D QSAR model can be used to design new *Trypanosoma cruzi* inhibitor.

REFERENCES

- [1] H. Jamal, W.H.Ansari, S. J. Rizui, <http://www.biomedonline.com>, *biology & medicine*, **2009**, 1(2), 107-115.
- [2] R. Pink, A.Hudson, M. A. Mouries, M. Bending, www.nature.com/reviews/drug-discovery, **2005**, 4, 727-740.
- [3] J. Diego Maya, B. K. Cassels, P. I. Vásquez, J. Ferreira, M. Faúndez, N. Galanti, A. Ferreira, A. Morello, **2007**, 146, 601-620.
- [4] C. A. Sotriffer, R. H. Winger, K. R. Winger, Rode Bernd M., Varga, *J. Comp. Aided Mol. Des.*, **1996**, 10, 305-320.
- [5] S. S. Narkhede, M. S. Degani, *QSAR Comb. Sci.*, **2007**, 26, 744–753.
- [6] S. Vepuri, N. R. Tawari, M. S. Degani, *QSAR Comb. Sci.*, **2007**, 26, 204–214.
- [7] S. Ramar, S. Bag, N. R. Tawari, M. S. Degani, *QSAR Comb. Sci.*, **2007**, 26, 608–617.
- [8] V. Hariprasad, V. M. Kulkarni, *J. Comp. Aided Mol. Des.*, **1996**, 10, 284.
- [9] Jose´ C. Aponte, Manuela Vera´stegui, Edith Ma´laga, Mirko Zimic, Miguel Quiliano, Abraham J. Vaisberg, Robert H. Gilman, and Gerald B. Hammond, *J. Med. Chem.*, **2008**, 51, 6230-6234.
- [10] PHASE, Version 3.0, Schrödinger, LLC, NY2008.
- [11] Maestro, Version 8.5, Schrödinger, LLC, NY2008.
- [12] W. C. Still, A. Tempczyk, R.C. Hawley, T. Hendrickson, *J. Am. Chem. Soc.*, **1990**, 112, 6127.
- [13] N. R. Tawari, S. Bag & Mariam S. Degani; *J. Mol. Model.*: **2008**(14), 911–921.
- [14] D. B. Boyd, Successes of computer-assisted molecular design, in: Reviews in computational chemistry, VCH, New York, **1990**, 355–371.
- [15] W. Jing, S. Wang, S. Gao, X. Dai, Q. Qoo, *J. Chem. Inf. Model*, **2007**, 47(2), 613-625.
- [16] H. Dureja, V. Kumar, S. Gupta, A. K. Madan, *J. Theo. Comput. Chem.*, **2007**, 6(3), 435–448.
- [17] S. Wold, *Quant. Struct. Act. Relat.*, **1991**, 10, 191-193.